67. Computations of ^{57}Fe-NMR Chemical Shifts with the SOS-DFPT Method

by **Michael Bühl***

Organisch-Chemisches Institut, Universität Zürich, Winterthurerstr. 190, CH-8057 Zürich

and **Olga L. Malkina**

Computer Center, Faculty of Natural Sciences, Comenius University, Mlynska Dolina CH-1, SK-84215 Bratislava

and **Vladimir G. Malkin**

Institute of Inorganic Chemistry, Slovak Academy of Sciences, Dubravska cesta 9, SK-84236 Bratislava

(5.II.96)

^{57}Fe Shielding tensors of substituted iron-carbonyl complexes have been computed employing the density-functional-based SOS-DFPT method (sum-over-states density-functional perturbation theory) with the IGLO (individual gauge for localized orbitals) choice of gauge origins and with large basis sets. The shieldings computed for $[Fe(CO)_5]$, $[Fe(CO)_3(H_2C{=}CHCH{=}CH_2)]$, $[Fe(CO)_3(\text{cyclo-}C_4H_4)]$, $[Fe(CO)_4(H_2C{=}CHOMe)]$, $[Fe(CO)_4(H_2C{=}CHCN)]$, $[Fe(CO)_3(H_2C{=}CHCH{=}O)]$, and $[Fe(CO)_2(C_5H_5)R]$ (R = Me, Bu, i-Pr) correlate with the experimental $\delta(^{57}Fe)$ values. However, the slope of the correlation line is 0.55 instead of 1, *i.e.*, only about one half of the substituent effects on σ(Fe) is recovered in the calculations. Nearest-neighbor effects appear to be described qualitatively (*cf.* in the $[Fe(CO)_2(C_5H_5)R]$ series, whereas effects of more remote substituents, *e.g.*, for $[Fe(CO)_4(H_2C{=}CHX)]$ (X = MeO and CN)) are not reproduced. Dissociation energies of these species are discussed because of their relevance to experimental rate constants for substitution processes which are known to correlate with $\delta(^{57}Fe)$. Even though the $\delta(^{13}C)$ and $\delta(^{1}H)$ data of ferrocene (**7**) are well reproduced theoretically, the computed σ(Fe) shielding of **7** deviates substantially from the σ(calc.)/δ(expt.) correlation, possibly indicating additional shortcomings in the theoretical description of this molecule.

Introduction. – While more and more nuclei of the periodic table can feasibly be treated in chemical-shift computations [1–3], NMR properties of transition-metal compounds remain a challenge for theory [4]. One reason is the need to go beyond the SCF approximation, in particular for species involving elements from the first transition row. Among these, it is only for the early and the post-transition metals where qualitatively correct descriptions of chemical shifts can be obtained at SCF level, *e.g.*, for Ti [5] and Zn [6] species. The size of compounds of practical interest usually precludes the use of sophisticated electron-correlated methods such as GIAO (gauge-including atomic orbitals)-MP2 [7], GIAO-CCSD [8], or multiconfigurational methods [9] [10].

Methods based on density functional theory (DFT) [11] [12] would offer a promising alternative. Among the approaches developed and implemented recently, SOS-DFPT-IGLO (sum-over-states density-functional perturbation theory with individual gauges for localized orbitals) [13] [14] and GIAO-DFT [15] have been most extensively applied to date. Very recently, a current-density functional (CDFT) method has been implemented employing GIAOs [16]. The results for lighter, but also for heavier main-group elements, are usually surpassing the corresponding SCF data in accuracy, *i.e.*, in the degree of

agreement with experiment. It is most noteworthy that ^{13}C, ^{17}O, as well as ^{31}P chemical shifts of ligands in the coordination sphere of transition-metal compounds are described very well with the SOS-DFPT method in conjunction with effective core potentials on the metal atom [17–21]. Thus, one would expect that the chemical shifts of the transition metals themselves should be computed equally well (provided all electrons of the metal are treated explicitly). In a recent review on the use of chemical shift calculations in protein structure elucidation, confidence has been expressed that 'using DFT methods [...], the shifts of metal ions, such as those of ^{57}Fe or ^{113}Cd, should also be accessible' [22]. We now report results of ^{57}Fe chemical-shift calculations for several ion-carbonyl complexes which suggest that the expectations regarding the performance of DFT-based methods for transition-metal chemical-shift calculations may have been somewhat too optimistic, at least for middle to late 3d metals such as Fe.

The choice of test molecules has been motivated by recent findings that the $\delta(^{57}Fe)$ values of $[Fe(CO)_4(olefin)]$ and $[Fe(CO)_2(C_5H_5)(alkyl)]$ complexes can be correlated with kinetic parameters of certain substitution and insertion reactions, respectively [23] [24]. We have become interested in exploring theoretically the mechanisms by which the substituents affect the corresponding ground-state properties and activation parameters, apparently in a parallel way.

Results and Discussion. – *Geometries.* The molecules of this study, pentacarbonyliron (**1**), iron-olefin complexes **2–5**, and iron-cyclopentadienyl complexes **6** and **7** are displayed in *Fig. 1*, together with key structural parameters. Many of these complexes have been characterized by X-ray structure analysis, but accurate gas-phase geometries – which optimized geometries should be compared with – are scarce. For $[Fe(CO)_5]$ (**1**), $[Fe(CO)_4(H_2C{=}CH_2)]$ (**2a**), $[Fe(CO)_3(cyclo\text{-}C_4H_4)]$ (**4**), as well as for ferrocene (**7**), the computed geometrical parameters are in good accord with the experimental gas-phase electron-diffraction (GED) data [25–28], and are within the experimental uncertainties (which are fairly large in most cases).

A more accurate, microwave(MW)-derived geometry has recently been reported for $[Fe(CO)_3(H_2C{=}CHCH{=}CH_2)]$ (**3**) [29]. While computed and experimental Fe–C distances are in good accord, the theoretical C–C bond lengths of the complexed butadiene moiety differ substantially from the MW values: the computed r(C(1)–C(2)) and r(C(2)–C(3)) distances (corresponding to the double and single bonds, respectively, in free butadiene) are 1.435 and 1.426 Å, respectively, whereas the corresponding experimental data are 1.385(7) and 1.409(1) Å, respectively. Due to the somewhat lower precision of the former value, however, both MW-derived distances are nearly equal, within experimental error [30], and the r(C(1)–C(2)) MW distance is probably slightly too small. The theoretical values agree somewhat better with the X-ray-derived distances, 1.46 (±0.05) and 1.45 (±0.06) Å, respectively [31], and are consistent with equalized bond lengths in solution, as inferred from virtually identical ^1J(C,C) values [32]. Note also that the DFT, X-ray, and MW techniques yield different parameters, r_e, r_g, and r_z values, respectively (see *e.g.* [33]).

No experimental structure data are available for the cyclopentadienyl complexes **6a–c** (for the discussion of certain structural aspects, see below). For consistency, the optimized geometries, rather than experimental ones, have, therefore, been employed in the chemical-shift calculations for all compounds **1–7**.

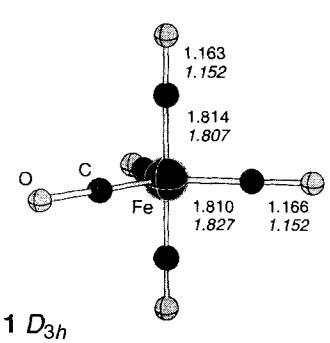

1 D_{3h}

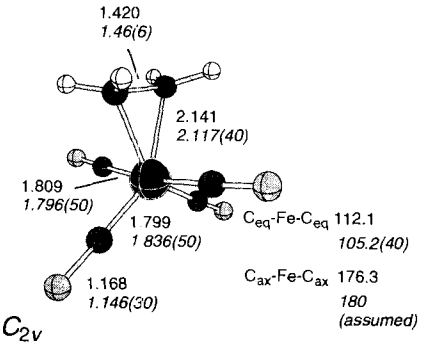

2a C_{2v}

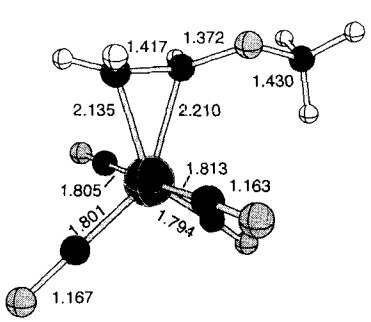

2b C_1

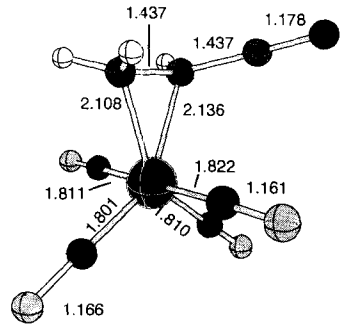

2d C_1

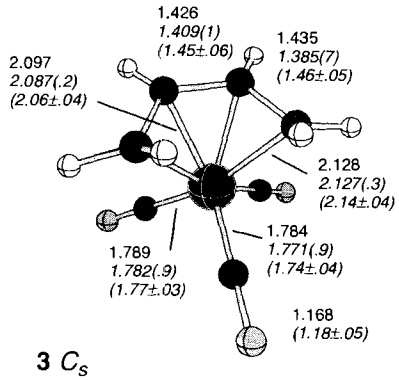

3 C_s

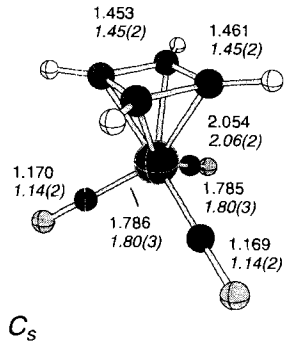

4 C_s

Fig. 1. *BP86/AE1-Optimized geometries for complexes* **1–7** *including key geometrical parameters in Å* (in italics: experimental gas-phase values from [25–28], in brackets: X-ray data from [31])

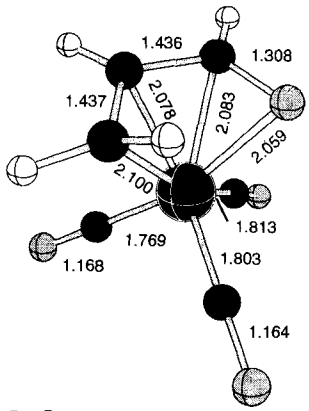

5 C_1

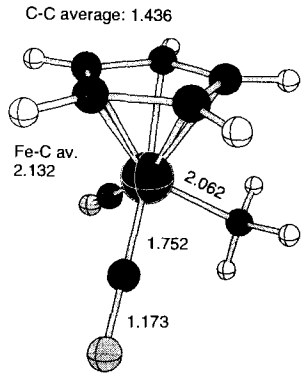

6a C_s

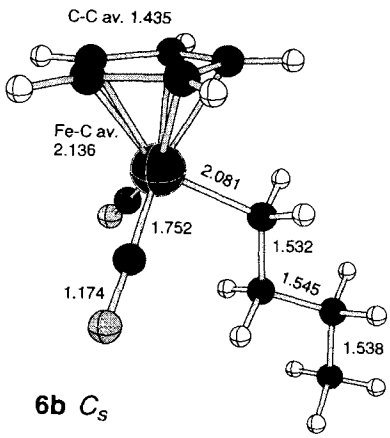

6b C_s

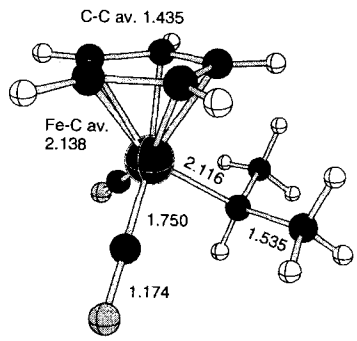

6c C_s

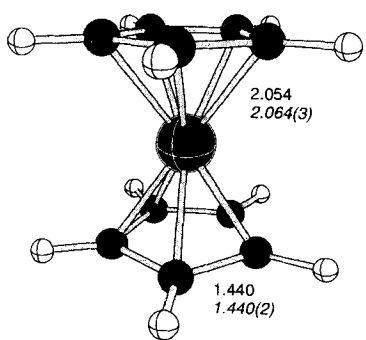

7 D_{5h}

Fig. 1 (cont.)

Table 1. *SOS-DFPT-Computed $\sigma(^{57}Fe)$ and Experimental $\delta(^{57}Fe)$ Values* (in ppm) *of Compounds* **1–7**

Compound		σ(II)[a])	σ(III)[b])	δ(exp.)[c])
$[Fe(CO)_5]$	**1**	–1592 [–1619]	–1796 (–1870)	0
$[Fe(CO)_4(H_2C{=}CH_2)]$	**2a**	–1509	–1709	–
$[Fe(CO)_4(H_2C{=}CHOMe)]$	**2b**	–1691	–1892	5[d])
$[Fe(CO)_4(H_2C{=}CHCN)]$	**2d**	–1694	–1887	303[d])
$[Fe(CO)_3(H_2C{=}CHCH{=}CH_2)]$	**3**	–1479 [–1439]	–1656	4
$[Fe(CO)_3(cyclo\text{-}C_4H_4)]$	**4**	–1147	–1312 (–1426)	–583
$[Fe(CO)_3(H_2C{=}CHCH{=}O)]$	**5**	–2219	–2417 (–2518)	1274
$[Fe(CO)_2(C_5H_5)CH_3]$	**6a**	–1878	–2052[e])	684[f])
$[Fe(CO)_2(Bu)(C_5H_5)]$	**6b**	–1937	–2116[e])	716[f])
$[Fe(CO)_2(C_5H_5)(i\text{-}Pr)]$	**6c**	–1993	–2175[e])	796[f])
$[Fe(C_5H_5)_2]$	**7**	–1725 [–1836]	–1837 (–2057)	1532

[a]) Basis II for BP86 geometries; in brackets, results for experimental geometries. [b]) Basis III for BP86 geometries; in parentheses, basis IV data, see text. [c]) From [39] except where otherwise noted. [d]) From [23]. [e]) For H-atoms, basis III only on α-H-atoms of the alkyl chain, basis II for the other H-atoms. [f]) From [24].

^{57}Fe Chemical Shifts. The isotropic ^{57}Fe shieldings σ, computed with the SOS-DFPT method employing two basis sets and the optimized DFT geometries, are summarized in *Table 1*, together with the experimental $\delta(^{57}Fe)$ data. In principle, theoretical chemical shifts can be computed directly relative to $[Fe(CO)_5]$ (**1**), the experimental standard. Since **1** is highly fluxional on the NMR time scale [34], the static equilibrium structure may not be a suitable theoretical model for this standard. Therefore, the computed absolute shieldings σ have been plotted directly *vs.* the experimental δ values in *Fig. 2*. Except for

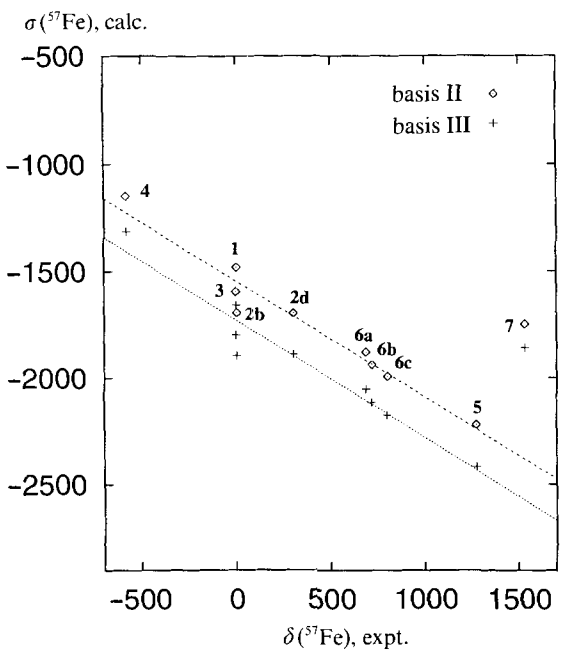

Fig. 2. *Plot of computed ^{57}Fe magnetic shieldings σ vs. experimental $\delta(^{57}Fe)$ chemical shifts.* The slope of the regression line (excluding **7**) is 0.55 for both basis sets.

ferrocene (**7**; see below), there are fairly good linear correlations, σ(calc.) *vs.* δ(expt.), for both basis sets. However, the slopes of the regression lines are not unity, as they should be, but are only 0.55 in both cases. Thus, only about half of the substituent effects on σ(Fe) are recovered by the SOS-DFPT calculations.

The notable differences in the computed σ values for the two basis sets, on average nearly 200 ppm, suggest that the basis is still not fully saturated. However, in going from basis II to basis III, the correlation line in *Fig. 2* is merely shifted, its slope remaining unchanged. It seems, therefore, unlikely that further enlargement of the spd basis would improve the results in terms of the shift range covered. Some specific test calculations with larger spd basis sets on iron (basis IV) and also with finer integration grids have corroborated this conclusion: *e.g.*, the computed shift difference between the two 'extreme cases' of this study, **4** and **5**, is practically unaffected when going from basis III ($\Delta\delta \approx 1100$ ppm) to basis IV ($\Delta\delta \approx 1090$ ppm; *cf.* the values in parentheses in *Table 1*). The same is found when the uncoupled DFT scheme (instead of SOS-DFPT) and/or a common gauge origin (instead of the IGLO choice) are employed, or when other local (*Vosko et al.* [35]) or non-local (*Becke* [36] and *Perdew* [37]) functionals are used.

For technical reasons, f-functions cannot yet be included in the basis set. Such f-functions would serve to polarize d-type orbitals. For 4th row elements with filled d-shells such as ^{77}Se, inclusion of f-functions does not affect the computed chemical shifts drastically [38]. This might be different for transition metals, but it is hardly conceivable that these higher polarization functions could have such dramatic effects as to double the computed shielding range.

The SOS-DFPT results for ferrocene (**7**) are particularly disappointing as they do not even fit into the correlations discussed above (see *Fig. 2*). With both basis II and III, σ(^{57}Fe) of **7** is computed *ca.* 500 ppm too large, *i.e.*, too strongly shielded, as would be expected from the correlation lines of compounds **1**–**6**. The computed differences in the isotropic shieldings of **7** and [Fe(CO)$_5$] (**1**), the experimental standard, is only *ca.* +150 ppm, whereas the corresponding experimental δ(^{57}Fe) value is +1532 ppm [39]. Inspection of the calculated principal value σ_{ii} and anisotropies $\Delta\sigma$ of the shielding tensors in *Table 2* reveals that **7** has by far the largest $\Delta\sigma$ value of all compounds studied here, more

Table 2. *SOS-DFPT-Computed*[a]) *Principal Values* σ_{ii} *and Anisotropies* $\Delta\sigma$ *of the* ^{57}*Fe Shielding Tensors*

Compound		σ_{11}[b])	σ_{22}	σ_{33}	$\Delta\sigma$[c])
[Fe(CO)$_5$]	**1**	–2041	–1679	–1669	–367
[Fe(CO)$_4$(H$_2$C=CH$_2$)]	**2a**	–1970	–1935	–1221	–787
[Fe(CO)$_4$(H$_2$C=CHOMe)]	**2b**	–2267	–1983	–1425	–563
[Fe(CO)$_4$(H$_2$C=CHCN)]	**2d**	–2281	–2019	–1361	–592
[Fe(CO)$_3$(H$_2$C=CHCH=CH$_2$)]	**3**	–2470	–1395	–1103	–1221
[Fe(CO)$_3$(cyclo-C$_4$H$_4$)]	**4**	–1571	–1204	–1162	–389
[Fe(CO)$_3$(H$_2$C=CHCH=O)]	**5**	–3517	–2493	–1240	–1650
[Fe(CO)$_2$(C$_5$H$_5$)CH$_3$]	**6a**	–2409	–2390	–1356	–536
[Fe(CO)$_2$(Bu)(C$_5$H$_5$)]	**6b**	–2512	–2427	–1411	–593
[Fe(CO)$_2$(C$_5$H$_5$)(i-Pr)]	**6c**	–2484	–2464	–1576	–465
[Fe(C$_5$H$_5$)$_2$]	**7**	–3235	–3225	950	4180

[a]) Basis III for BP86 geometries, in ppm. [b]) Ordering $\sigma_{11} < \sigma_{22} < \sigma_{33}$. [c]) Definition: $\sigma_{11} - (\sigma_{22} + \sigma_{33})/2$, for axially symmetric molecules **1** and **7**: $\sigma_{\parallel} - \sigma_{\perp}$.

than 4000 ppm. The component parallel to the molecular C_5 axis is exceptionally shielded; it is the only positive, *i.e.*, diamagnetic, value in this set. The absence of notable paramagnetic contributions in that direction is consistent with the qualitative MO picture [40]: no suitable occupied and virtual MO pairs are available that have large coefficients on Fe perpendicular to the C_5 axis (which would be required for such paramagnetic contributions). The lowest unoccupied orbitals are ligand-based and would have the proper symmetry for overlap with f-type orbitals on Fe. It might thus be possible that f-functions on Fe would improve the description of the magnetically induced orbital mixing that gives rise to paramagnetic shielding contributions. As mentioned above, however, it is unlikely that such polarization functions would have very large effects on the computed shieldings.

Despite the rather poor description of the ^{57}Fe shieldings in general, and that of **7** in particular, the results for ligand chemical shifts in the same complexes are in good accord with experiment (*cf.* for example $\delta(^{13}C)$ of **7**, computed 73.2 ppm (basis IV) *vs.* expt. 68.1 ppm (*e.g.* [41]), or $\delta(^{1}H)$, computed 3.9 *vs.* expt. 4.0 ppm). This degree of agreement is typical for theoretical chemical shifts of ligands in transition-metal complexes [17–21].

Geometry effects on $\delta(^{57}Fe)$ are notable, but are relatively small compared to the chemical-shift range. For **1**, **3**, and **7**, SOS-DFPT computations have been performed employing experimental gas phase, rather than optimized structures (values in brackets, *Table 1*). The largest effect, nearly 100 ppm, is found for ferrocene (**7**), but the computed ^{57}Fe chemical shift relative to **1** is only marginally improved, when the experimental geometries are employed, 217 ppm *vs.* expt. 1532 ppm.

At present, one may only speculate about the reasons of the rather poor performance of the SOS-DFPT method for ^{57}Fe chemical shifts. With the IGLO choice for the gauge origins, the diamagnetic contributions to σ(Fe) account at most for 25% of the theoretical chemical-shift range (the largest computed variation in σ_d is *ca.* 300 ppm). Thus, it is the paramagnetic part, σ_p, which appears to be insufficiently described with the theoretical model employed. This may indicate that the local and non-local functionals that have been employed do not satisfactorily describe the local excitations on the Fe-atom. These excitations should be crucial for the ^{57}Fe nucleus, but should be of less importance for the ligands. In this context, it is interesting to note that promotion energies of bare transition-metal atoms or ions, such as s–d excitation energies, are usually not well described with present DFT methods (see *e.g.* [42–44]).

Correlations between $\delta(^{57}Fe)$ and Reactivities. Relationships between the metal chemical shifts of transition-metal complexes and kinetic parameters, *e.g.* rate constants of substitution reactions or even catalytic activities, are of great potential interest. Many such examples have been documented, in particular by *v. Philipsborn* and coworkers [23] [24] [45–47]. Two recent cases have stimulated much of the present work: it has been shown that $\delta(^{57}Fe)$ of $[Fe(CO)_4(H_2C{=}CHX)]$ complexes (X = EtO, Ph, Bu, COOMe, CN) correlates with $\log k_{diss}$ of the olefin dissociation [23], and that $\delta(^{57}Fe)$ of a number of $[Fe(CO)_2(C_5H_5)R]$ species (R = alkyl) varies regularly with the rate constants of the PPh_3-induced CO insertion into the Fe–C(alkyl) bond [24]. Apparently, in these and other cases, the various substituents affect the chemical shifts of the central metal atom and the activation parameters of the rate-determining reactions in a similar, parallel way. There is no *a priori* relationship between these properties which are associated with different parts of the potential-energy surface, namely minima and transition structures.

We have become interested in exploring theoretically the mechanisms by which the substituents may affect these properties.

The first of the aforementioned reactions appeared especially attractive for a computational investigation, since a dissociative mechanism has been inferred experimentally [48], *i.e.*, the dissociation of the olefin (*Reaction 1*) is the rate-determining step.

$$[Fe(CO)_4(H_2C{=}CHX)] \xrightarrow{k_{diss}} [Fe(CO)_4] + H_2C{=}CHX \quad (1)$$

$$[Fe(CO)_4] + L \xrightarrow{fast} [Fe(CO)_4L], \quad L = CO, SbPh_3 \quad (2)$$

For various X, $\log k_{diss}$ has been shown to correlate with the corresponding $\delta(^{57}Fe)$ data of the reactants [23]. For the 'extreme' cases, X = EtO and X = CN, the experimental k_{diss} values cover *ca.* 3 orders of magnitude [23] [48], while $\delta(^{57}Fe)$ varies by nearly 300 ppm (see *Table 3* for the data). From simple transition-state theory [49] – assuming constant preexponential factors – one can estimate that relative rate constants differing by a factor of 1000 would correspond to changes in activation enthalpies of *ca.* 4 kcal/mol (at 40°, the temperature of the kinetic measurements). For a purely dissociative mechanism, the activation energy is essentially equal to the dissociation energy of the olefin. We have, therefore, been interested to see if the DFT methods employed would predict similar trends in the dissociation energies of the reactants as have been found for the rate constants.

Table 3. *Experimental Rate Constants* k_{diss} ($s^{-1}\,mol^{-1}$)[a]) *and Computed Dissociation Energies* ΔE_{diss} (kcal/mol) *for [Fe(CO)$_4$(olefin)] Species*

Olefin	$k_{diss}(CO)$ (k_{rel})	$k_{diss}(SbPh_3)$ (k_{rel})	ΔE_{diss}[b])
$H_2C{=}CH_2$			36.1 (33.1)
$H_2C{=}CHOEt$	$4\cdot10^{-4}$ (400)	$4\cdot10^{-4}$ (2000)	
$H_2C{=}CHOMe$			34.9 (32.2)
$H_2C{=}CHCN$	$9\cdot10^{-7}$ (1)	$2\cdot10^{-7}$ (1)	33.5 (31.1)

[a]) For olefin substitution with CO and $SbPh_3$, respectively, from [23] [48]. For purely dissociative mechanisms, both sets of values should be identical; the data for $SbPh_3$, obtained in homogenous solution, should be more reliable than those for CO which involve a heterogenous reaction.

[b]) D_e Values at the BP86/AE1 level; in parentheses, with inclusion of the BP86/AE1 zero-point correction (unscaled).

At the BP86/AE1 level, the first CO dissociation energy of $[Fe(CO)_5]$ is 49.0 kcal/mol [50], which decreases to 46.2 kcal/mol upon inclusion of zero-point corrections. The latter value is in good agreement with other recent theoretical results at nonlocal DFT [51] and MP2 levels [52], and is in fairly good accord with the experimental estimate of 42 kcal/mol [53] (the theoretical data refer to the excited $^1A_1$ singlet state of $[Fe(CO)_4]$, as do most probably the experimental results; the $^3B_2$ triplet ground state has been computed *ca.* 2 kcal/mol below $^1A_1$ at nonlocal DFT levels). At the same level, BP86/AE1 + ZPE, the computed energy for ethylene dissociation from $[Fe(CO)_4(H_2C{=}CH_2)]$ (**2a**) is 33.1 kcal/mol. Thus, a considerable thermodynamic driving force, −12.9 kcal/mol, is com-

puted for the substitution (*Reaction 3*), consistent with the fact that CO readily replaces olefins in compounds of the type **2**.

$$[Fe(CO)_4(H_2C{=}CH_2)] + CO \longrightarrow [Fe(CO)_5] + H_2C{=}CH_2 \qquad (3)$$

Computed substituent effects on the olefin dissociation energy ΔE_{diss} of **2a** are given in *Table 3*. Somewhat counterintuitively, replacing one olefin H-atom by either an electron-donating (MeO, **2b**, serving as a model for **2c**, the actual compound with an EtO group) or an electron-withdrawing substituent (CN, **2d**) reduces the predicted ΔE_{diss} values, albeit only by *ca.* 1–2 kcal/mol. In contrast to the expectations mentioned above, the theoretical ΔE_{diss} values of **2b** and **2d** are quite close to each other, within *ca.* 1 kcal/mol. Thermal corrections, computed from the harmonic vibrational frequencies, are identical for both **2b** and **2d**. ΔE_{diss} and, thus, ΔG_{diss} of **2b** is even predicted to be larger than that of **2d** even though the latter has the smallest experimental k_{diss} value. Several reasons for this apparent inconsistency are conceivable. First, **2c** and **2d** might follow different reaction mechanisms. In fact, the kinetic studies revealed significantly different entropies of activation, namely -19 and $+16$ $calK^{-1}mol^{-1}$ for **2c** and **2d**, respectively [48], suggesting that the substitution mechanism of the vinyl ether may not be purely dissociative. Second, solvation energies might be important; *e.g.*, the more polar CN derivative **2d** could be more strongly stabilized by solvent interactions than **2b**, which would result in an increase of the effective ΔE_{diss} of **2c** relative to **2a**. Indeed, the computed (BP86/AE1) dipole moment of **2d**, 3.5 D, is somewhat larger than that of **2b**, 2.8 D. It is unlikely, however, that toluol, the solvent used in the measurements, would induce a significant differentiation between the two compounds. Finally, the theoretical model employed might not adequately describe the 'indirect' effects of remote substituents on the Fe–olefin bonding. Similar shortcomings are apparent in the ^{57}Fe chemical-shift calculations: despite the large experimental difference in $\delta(^{57}Fe)$ between **2c** and **2d** (*ca.* 300 ppm) [23], almost identical isotropic shieldings are computed for the model **2b** and **2d** (see *Tables 1* and *3* for the data). Relative to the parent **2a**, both MeO and CN substituents at the olefin are computed to decrease the ^{57}Fe shielding by *ca.* 180 ppm. Theoretical investigations of 'remote substituent' effects on chemical shifts and reactivities of other transition-metal compounds are in progress in order to identify systems that are better suited for the present approach.

Another relation between $\delta(^{57}Fe)$ and reactivities has been found for $[Fe(CO)_2(C_5H_5)R]$ (R = alkyl) complexes: with increasing bulkiness of R, *e.g.* in the series Me (**6a**), Bu (**6b**), i-Pr (**6c**), the ^{57}Fe-nucleus becomes more deshielded; at the same time, the CO insertion into the Fe–C(alkyl) bond according to *Eqn. 4* proceeds more facile [24].

$$[Fe(CO)_2(C_5H_5)R] + L \xrightarrow{k_{obs}} [Fe(CO)(C_5H_5)L(-\overset{\overset{O}{\|}}{C}-R)], \quad L = PPh_3 \qquad (4)$$

It has been suspected that the Fe–C(alkyl) bond strength decreases with increasing steric demand of R, which should eventually facilitate CO insertion. Different Fe–C(alkyl) bond strengths should also be reflected in the $\delta(^{57}Fe)$ chemical shifts. Similar steric effects on transition-metal chemical shifts have been noted, *e.g.* for Co complexes [54].

A first indicator for the strength of a Fe–C(alkyl) bond should be its length. Except for special cases [55], stronger bonds are associated with shorter bond distances. X-Ray

structures of $[Fe(CO)_2(C_5H_5)R]$ derivatives are available only for highly substituted and/or polycyclic species, but not for any of the compounds investigated. Therefore, representative molecules **6a–c** have been geometry-optimized at the BP/AE1 level. Since the metal–ligand separations of complexes **1–4** and **7** are described rather well at that level (see *Geometries* above), reliable trends for the Fe–C(alkyl) bond lengths should be predicted for **6a–c**.

Inspection of the geometrical data in *Fig. 1* confirms the expectations expressed above: the computed Fe–C(alkyl) bond lengths for **6a**, **6b**, and **6c** are 2.062, 2.081, and 2.116 Å, respectively, *i.e.*, an increase in bulkiness of R is paralleled by a significant Fe–C(alkyl) bond elongation (*e.g.* more than 5 pm in going from **6a** to **6c**). A frequency calculation has confirmed that **6a** is a true minimum. For **6c**, another rotamer has been optimized in C_1 symmetry (i-Pr group rotated *ca.* 120° about the Fe–C bond); this form is computed by *ca.* 0.3 kcal/mol above the one depicted in *Fig. 1* and has a similar Fe–C(propyl) bond length, 2.119 Å.

How do the relative bond elongations translate into relative bond strengths? In principle, bond dissociation energies (*BDE*s) can be computed directly according to *Eqn. 5*:

$$[Fe(CO)_2(C_5H_5)R] \rightarrow \dot{F}e(CO)_2(C_5H_5) + R\cdot \quad D_e = \begin{matrix} 51.9\ \text{kcal/mol (R = Me)} \\ 46.9\ \text{kcal/mol (R = Bu)} \\ 40.8\ \text{kcal/mol (R = i-Pr)} \end{matrix} \qquad (5)$$

Indeed, substantial variations in the *BDE*s are predicted. (In principle, DFT methods for open-shell systems should employ spin-unrestricted rather than spin-restricted formulations, see *e.g.* [56]. When the UBP86, rather than the ROBP86 method is used, the computed D_e values according to *Eqn. 5* are 49.6, 44.7 and 38.6 kcal/mol, *i.e.*, the same trend is predicted.) Energies of reactions involving multiplicity changes are difficult to compute exactly. Due to more favorable error compensations, isogyric reactions (*i.e.*, reactions with conservation of multiplicity) are easier to describe theoretically [57]. *Eqn. 6* relates the *BDE*s of the Fe–C(alkyl) bonds to those of the C–H bonds in the corresponding alkanes.

$$[Fe(CO)_2(C_5H_5)R] + H\cdot \rightarrow \dot{F}e(CO)_2(C_5H_5) + R{-}H \quad \Delta E = \begin{matrix} -63.5\ \text{kcal/mol (R = Me)} \\ -63.3\ \text{kcal/mol (R = Bu)} \\ -64.9\ \text{kcal/mol (R = } i\text{Pr)} \end{matrix} \qquad (6)$$

The driving forces are very similar in each case, indicating parallel trends and comparable variations in the $[Fe(CO)_2(C_5H_5)R]$ and H–R *BDE*s. The experimental D_o values for the latter vary between 103.3 (Me–H) and 97.1 kcal/mol (i-Pr–H) [58]. The computations thus predict a decrease in the Fe–C(alkyl) *BDE* of at least 6 kcal/mol in going from R = Me to R = i-Pr. It is reasonable to assume that the barrier for CO insertion decreases with the bond energy; a theoretical confirmation, however, would require full optimizations of the corresponding transition states.

The trend in the $\delta(^{57}Fe)$ values of **6a–c** is well reproduced computationally (*cf.* the $\Delta\delta$ values relative to **6a**, 65 and 123 ppm for **6b** and **6c**, respectively (basis III) *vs.* experiment, 32 and 112 ppm, respectively; see *Table 1*). In view of the SOS-DFPT results for the other compounds of this study (see above), the good description of the chemical-shift range in the subset **6a–c** may be somewhat fortuitous. The trend for **6a–c** may be rationalized in terms of the localized MO (LMO) contributions: The deshielding of $\sigma(^{57}Fe)$ in this series

is largely due to changes in the LMO contribution of the Fe–C(alkyl) σ-bond, which becomes more paramagnetic in character by 64 and 88 ppm in going from **6a** to **6b** and **6c**, respectively. Only part of the deshielding of **6b** and **6c** relative to **6a** appears to originate from steric effects: When the Fe–CH_3 bond length in **6a** is set to the corresponding Fe–C(alkyl) distance in **6b** and **6c** (leaving all other parameters unchanged), deshieldings of 18 and 52 ppm, respectively, are computed (basis II).

Conclusions. – Geometries and ^{57}Fe chemical shifts of iron complexes with CO, olefin, cyclopentadienyl, and alkyl ligands have been computed at gradient-corrected DFT levels. In general, available experimental gas-phase geometries are well reproduced at the BP86 level with a medium-sized set. Absolute ^{57}Fe shieldings, computed with the SOS-DFPT method and large basis sets, correlate with experimental $\delta(^{57}Fe)$ data. However, the slope of the regression line is only 0.55 instead of unity, *i.e.*, only about half of the substituent effects on $\delta(^{57}Fe)$ is recovered in the calculations. Additional shortcomings are apparent for the theoretical chemical shift of ferrocene (**7**) which deviates by more than 1300 ppm from the experimental data.

For $[Fe(CO)_4(H_2C{=}CHX)]$ (X = MeO (**2b**) and CN (**2c**)), the computed olefin dissociation energies are very similar and do not agree with the large variations of the experimental rate constants for dissociative substitution. Likewise, the computed ^{57}Fe chemical shifts of **2b** and **2c** are virtually identical and fail to reproduce the substantial difference in the corresponding experimental data, *ca.* 300 ppm.

For $[Fe(CO)_2(C_5H_5)R]$ (R = Me (**6a**), Bu (**6b**), and i-Pr (**6c**)), on the other hand, computed trends in the Fe–C(alkyl) bond dissociation energies are consistent with the experimental rate constants for phosphine-induced CO insertion into these bonds. Both direction and magnitude of the changes in $\delta(^{57}Fe)$ with R are well described with the SOS-DFPT method. It appears that the currently employed DFT methods and functionals can qualitatively describe substituent effects on transition-metal chemical shifts and, possibly, on reactivities when the substituents are directly attached to the metal, as in **6a–c**. The corresponding effects of more remote substituents, as in **2b** and **2d**, seem to be grossly underestimated. Investigations are in progress for other transition-metal complexes in order to further explore the possibilities and limitations of the present theoretical models in describing substituent effects on transition-metal chemical shifts and activation parameters.

Computational Details. – Geometries have been fully optimized in the given symmetry with the G92/dft [59] and G94 [60] program packages at a gradient-corrected DFT level employing *Becke*'s 1988 exchange [36] and *Perdew*'s 1986 [37] correlation functionals, a 'fine' integration grid ('finegrid' option), *Wachters*' (14s11p6d)/[8s7p4d] all-electron basis augmented with one additional diffuse d and two 4p functions for Fe [61] [62], and 6-31G* basis set [57] for the ligands. Geometries and vibrational frequencies of a number of transition-metal carbonyls have been shown to agree very well with experiment at that level (designated BP86/AE1) [50]. In some cases, harmonic frequency calculations have been performed in order to compute zero-point and thermal corrections (see text). For the bond-strength evaluations, open-shell species have been treated in the restricted open-shell approximation (designated ROBP86).

Shielding tensors have been computed for the optimized geometries using the sum-over-states density-functional perturbation theory (SOS-DFPT) approach [13] [14] in its LOC1 approximation and individual gauges for localized orbitals (IGLO) [1] [63] [64], as implemented in the deMon program [65] [66]. *Perdew* and *Wang*'s 1991 exchange-correlation functional [67] [68] has been employed, together with a 'fine' integration grid ('FINE' option) and the following basis sets: basis II: same augmented *Wachters* basis as above for Fe, and IGLO-II basis [1] for the ligands, *i.e.*, (9s5p)/[5s4p] augmented with one set of d-polarization functions for C, N, O, and (5s)/[3s] augmented with one set of p-polarization functions for H; basis III: same *Wachters* basis as above, but decontracted to

[10s9p5d] and equally augmented for Fe, and IGLO-III basis for the ligands, *i.e.*, (11s7p)/[7s6p] augmented with two sets of d functions for C, N, O, and (6s)/[4s] augmented with two sets of p functions for H. Auxiliary basis sets of the type (5,5) for Fe, (5,2) for C, N, O, and (5,1) for H have been used for the fit of the exchange-correlation potential and of the charge densities (*n,m* stands for *n* s-functions and *m* spd-shells). For the ligands, basis II and auxiliary basis sets are the same as have been used in the $\delta(^{13}C)$ and $\delta(^{17}O)$ chemical shift computations of transition-metal complexes [17–21]. In addition, some test calculations have been performed employing basis IV, *i.e.*, a large uncontracted 24s16p12d *Partridge* basis on iron [69] augmented with an additional spd set, together with basis II on the ligands and a finer integration grid (64 radial shells). With this basis, ^{13}C chemical shifts have been computed relative to TMS, for which we employed the experimental gas-phase geometry, a large 20s15p10d+spd basis from [69] for Si, and basis II for the CH_3 groups.

M. B. wishes to thank Prof. Dr. *W. Thiel* and the *Fonds der Chemischen Industrie* for support and Prof. *D. R. Salahub* for making the deMon program available. *O. L. M.* and *V. G. M.* gratefully acknowledge financial support from the *Slovak Grant Agency for Science* (grant No. 2/1172/96). This work has also benefited from the earlier *Alexander von Humboldt* fellowship of *V. G. M.* at the Ruhr-Universität Bochum. Comments and suggestions of Dr. *T. Clark*, Dr. *U. Fleischer*, and, in particular, Dr. *M. Kaupp* have been very helpful. We also thank Prof. Dr. *W. v. Philipsborn*, Dr. *M. Koller*, and *E. Meier* for stimulating discussions and for providing us with experimental data prior to publication. The calculations have been carried out on *IBM RS6000* workstations at the University and at the ETH-Zürich (C4 cluster), as well as on the *NEC-SX3* at the *CSCS* in Manno, Switzerland.

REFERENCES

[1] W. Kutzelnigg, U. Fleischer, M. Schindler, in 'NMR Basic Principles and Progress', Springer-Verlag, Berlin, 1990, Vol. 23, p. 165.
[2] G. A. Webb, in 'Nuclear Magnetic Shieldings and Molecular Structure', NATO ASI Series, Ed. J. A. Tossell, Kluwer, Amsterdam, 1993, p. 1.
[3] D. B. Chesnut, *Annu. Rep. NMR Spectrosc.* **1989,** *21,* 51.
[4] H. Nakatsuji, in 'Nuclear Magnetic Shieldings and Molecular Structure', Ed. J. A. Tossell, Kluwer Academics, Amsterdam, 1993, p. 263.
[5] S. Berger, W. Bock, G. Frenking, V. Jonas, F. Müller, *J. Am. Chem. Soc.* **1995,** *117,* 3820.
[6] J. A. Tossell, *Chem. Phys. Lett.* **1990,** *169,* 145.
[7] J. Gauss, *J. Chem. Phys.* **1993,** *99,* 3629.
[8] J. Gauss, J. F. Stanton, *J. Chem. Phys.* **1995,** *102,* 3561.
[9] C. v. Wüllen, W. Kutzelnigg, *Chem. Phys. Lett.* **1993,** *205,* 563.
[10] K. Ruud, T. Helgaker, R. Kobayashi, P. Jørgensen, K. L. Bak, J. J. A. Jensen, *J. Chem. Phys.* **1994,** *100,* 8178.
[11] J. M. Seminario, P. Politzer, Ed., 'Modern Density Functional Theory', Elsevier, Amsterdam, 1995.
[12] R. G. Parr, W. Yang, 'Density Functional Theory of Atoms and Molecules', Academic Press, Oxford, 1989.
[13] V. G. Malkin, O. L. Malkina, M. E. Casida, D. R. Salahub, *J. Am. Chem. Soc.* **1994,** *116,* 5898.
[14] V. G. Malkin, O. L. Malkina, L. A. Eriksson, D. R. Salahub, in 'Modern Density Functional Theory', Eds. J. M. Seminario and P. Politzer, Elsevier, Amsterdam, 1995, p. 273.
[15] G. Schreckenbach, T. Ziegler, *J. Chem. Phys.* **1995,** *99,* 606.
[16] A. M. Lee, N. C. Handy, S. M. Colwell, *J. Chem. Phys.* **1995,** *103,* 10095.
[17] M. Kaupp, V. G. Malkin, O. L. Malkina, D. R. Salahub, *Chem. Phys. Lett.* **1995,** *235,* 382.
[18] M. Kaupp, V. G. Malkin, O. L. Malkina, D. R. Salahub, *J. Am. Chem. Soc.* **1995,** *117,* 1851.
[19] M. Kaupp, V. G. Malkin, O. L. Malkina, D. R. Salahub, *Chem. Eur. J.* **1996,** *2,* 24.
[20] M. Kaupp, *Chem. Eur. J.* **1996,** *2,* 194.
[21] M. Kaupp, *Chem. Ber.*, in press.
[22] D. D. Laws, A. C. de Dios, E. Oldfield, *J. Biomol. NMR* **1993,** *3,* 607.
[23] M. Koller, Ph. D. Thesis, University Zurich, 1993.
[24] E. J. Meier, W. Kozminski, A. Linden, P. Lustenberger, W. v. Philipsborn, *Organometallics*, in press.
[25] B. Beagley, D. G. Schmidling, *J. Mol. Struct.* **1974,** *22,* 466.
[26] M. I. Davis, C. S. Speed, *J. Organomet. Chem.* **1970,** *21,* 401.
[27] H. Oberhammer, H. A. Brune, *Z. Naturforsch.* **1969,** *24,* 607.
[28] R. K. Bohn, A. Haaland, *J. Organomet. Chem.* **1996,** *5,* 470.

[29] S. G. Kukolich, M. A. Roehrig, D. W. Wallace, G. L. Henderson, *J. Am. Chem. Soc.* **1993,** *115,* 2021.
[30] S. G. Kukolich, private communication.
[31] Mills, Robinson, *Acta Crystallogr.* **1963,** *16,* 758.
[32] S. Zobl-Ruh, W. v. Philipsborn, *Helv. Chim. Acta* **1980,** *63,* 773.
[33] R. A. Beaudet, in 'Advances in Boron and the Boranes', Eds. J. F. Liebmann, A. Greenberg, and R. E. Williams, VCH Publisher, New York, 1988, Chapt. 20, p. 417.
[34] R. Bramley, B. N. Figgs, R. S. Nyholm, *Trans. Faraday Soc.* **1962,** *58,* 1893.
[35] S. H. Vosko, L. Wilk, M. Nusair, *Can. J. Chem.* **1980,** *58,* 1200.
[36] A. D. Becke, *Phys. Rev. A* **1988,** *38,* 3098.
[37] J. P. Perdew, *Phys. Rev. B* **1986,** *33,* 8882; *ibid.* **1986,** *34,* 7406.
[38] M. Bühl, W. Thiel, U. Fleischer, W. Kutzelnigg, *J. Phys. Chem.* **1995,** *99,* 4000.
[39] R. Benn, in 'Transition Metal Nuclear Magnetic Resonance', Ed. P. S. Pregosin, Elsevier, Amsterdam, 1991, p. 103.
[40] M. F. Rettig, in 'NMR of Paramagnetic Compounds, Principles and Applications', Eds. G. N. LaMas, J. W. DeW. Horrocks, and R. H. Holm, Academic Press, New York, 1973, p. 217.
[41] R. B. Materiovka, V. N. Babin, I. R. Lyatifov, T. K. Kurbanov, E. I. Fedin, P. V. Petrovskii, A. I. Lutsenko, *J. Organomet.* **1977,** *142,* 81.
[42] R. Fournier, *J. Chem. Phys.* **1993,** *99,* 1801.
[43] T. Ziegler, J. Li, *Can. J. Chem.* **1993,** *72,* 783.
[44] M. C. Holthausen, C. Heinemann, H. H. Cornehl, W. Koch, H. Schwarz, *J. Chem. Phys.* **1995,** *102,* 4931.
[45] V. Tedesco, W. v. Philipsborn, *Organometallics* **1995,** *14,* 3600.
[46] M. Koller, W. v. Philipsborn, *Organometallics* **1992,** *11,* 467.
[47] P. DeShong, D. R. Sidler, P. J. Rybczynski, A. A. Ogilvie, W. v. Philipsborn, *J. Org. Chem.* **1989,** *54,* 5432.
[48] C. Gordaci, V. Narcisco, *J. Chem. Soc., Dalton Trans.* **1972,** 2289.
[49] S. W. Benson, 'Thermochemical Kinetics', Wiley, New York, 1976.
[50] V. Jonas, W. Thiel, *J. Chem. Phys.* **1995,** *102,* 8474.
[51] J. Li, G. Schreckenbach, T. Ziegler, *J. Am. Chem. Soc.* **1995,** *117,* 486.
[52] A. Ehlers, G. Frenking, *Organometallics* **1995,** *14,* 423.
[53] K. E. Lewis, D. M. Golden, G. P. Smith, *J. Am. Chem. Soc.* **1984,** *106,* 3905.
[54] C. Tavagnacco, G. Balducci, G. Costa, K. Täschler, W. v. Philipsborn, *Helv. Chim. Acta* **1990,** *73,* 1469.
[55] R. D. Ernst, J. Freeman, L. Stahl, D. R. Wilson, A. M. Arif, B. Nuber, M. L. Ziegler, *J. Am. Chem. Soc.* **1995,** *117,* 5075.
[56] J. A. Pople, P. M. W. Gill, N. C. Handy, *Int. J. Quantum Chem.* **1995,** *56,* 303.
[57] W. J. Hehre, L. Radom, P. v. R. Schleyer, J. A. Pople, 'Ab initio Molecular Orbital Theory', Wiley, New York, 1986.
[58] J. Berkowitz, G. B. Ellison, D. Gutman, *J. Phys. Chem.* **1994,** *98,* 2744.
[59] M. J. Frisch, G. W. Trucks, H. B. Schlegel, P. M. W. Gill, B. G. Johnson, M. W. Wong, J. B. Foresman, M. A. Robb, M. Head-Gordon, E. S. Replogle, R. Gomperts, L. Andres, K. Raghavachari, J. S. Binkley, C. Gonzales, R. L. Martin, D. J. Fox, D. J. DeFrees, J. Baker, J. J. P. Stewart, J. A. Pople, Gaussian 92/DFT, Pittsburgh PA, 1993.
[60] M. J. Frisch, G. W. Trucks, H. B. Schlegel, P. M. W. Gill, B. G. Johnson, M. A. Robb, J. R. Cheeseman, T. Keith, G. A. Petersson, J. A. Montgomery, K. Raghavachari, M. A. Al-Laham, V. G. Zakrzewski, J. V. Ortiz, J. B. Foresman, C. Y. Peng, P. Y. Ayala, W. Chen, M. W. Wong, J. L. Andres, E. S. Replogle, R. Gomperts, R. L. Martin, D. J. Fox, J. S. Binkley, D. J. DeFrees, J. Baker, J. J. P. Stewart, M. Head-Gordon, C. Gonzales, J. A. Pople, Gaussian 94, Pittsburgh PA, 1995.
[61] A. J. H. Wachters, *J. Chem. Phys.* **1970,** *52,* 1033.
[62] P. J. Hay, *J. Chem. Phys.* **1977,** *66,* 4377.
[63] W. Kutzelnigg, *Isr. J. Chem.* **1980,** *19,* 193.
[64] M. Schindler, W. Kutzelnigg, *J. Chem. Phys.* **1982,** *76,* 1919.
[65] D. R. Salahub, R. Fournier, P. Mlynarski, I. Papai, A. St-Amant, J. Ushio, in 'Density Functional Methods in Chemistry', Ed. J. K. Labanowski and J. W. Andzelm, Springer, New York, 1991, p. 77.
[66] A. St-Amant, D. R. Salahub, *Chem. Phys. Lett.* **1990,** *169,* 387.
[67] J. P. Perdew, Y. Wang, *Phys. Rev. B* **1992,** *45,* 13244.
[68] J. J. Perdew, in 'Electronic Structure of Solids', Eds. P. Ziesche and H. Eischrig, Akademie Verlag, Berlin, 1991.
[69] H. Partridge, *J. Chem. Phys.* **1987,** *87,* 6643; *ibid.* **1989,** *90,* 1043.